## Terrain-Dependent Generalization Failure in Multimodal Lunar Crater Classification: A Comparative Study Using Optical and Topographic Data

Shreyas Khobragade

Vidyalankar Institute of Technology
Mumbai, Maharashtra, India

Corresponding Author:
shreyaskhobragade1002@gmail.com

ORCID:
0009-0008-8659-2970

---



---

September 8, 2026

# Terrain-Dependent Generalization Failure in Multimodal Lunar Crater Classification: A Comparative Study Using Optical and Topographic Data

Shreyas Khobragade

Vidyalankar Institute of Technology, Mumbai, India
ORCID: 0009-0008-8659-2970

***Abstract*—Automated lunar crater detection is an important task in planetary mapping, geological analysis, and future lunar exploration. Recent studies have demonstrated the potential of combining optical imagery with topographic information; however, the influence of terrain variability on crater classification performance remains insufficiently explored.**

**This study presents a comparative evaluation of optical imagery, Digital Terrain Model (DTM) data, and multimodal fusion strategies for lunar crater classification across geologically distinct lunar terrains. A manually curated dataset containing 1,904 image patches was developed from co-registered Lunar Reconnaissance Orbiter Camera (LROC) products covering Mare Tranquillitatis and the Tycho Highlands. Four classification approaches were evaluated using a common convolutional neural network architecture: Optical-only, DTM-only, Early Fusion, and Late Fusion models.**

**Experimental results showed that DTM-based classification slightly outperformed optical imagery, while both fusion approaches achieved performance comparable to the DTM model, yielding overall accuracies of approximately 76%. Terrain-wise evaluation revealed a more significant finding. Although all models achieved reasonable crater detection performance within Mare Tranquillitatis, every approach failed to identify crater samples within the Tycho Highlands subset.**

**Analysis of the curated dataset indicated that severe terrain-dependent sample imbalance and limited representation of highland crater morphologies exerted a stronger influence on performance than input modality or fusion strategy. These findings highlight the importance of terrain-balanced datasets for robust lunar crater classification and suggest that training data diversity may be as critical as advances in multimodal fusion methodology for achieving reliable cross-terrain generalization.**

***Index Terms*—Lunar crater classification, multimodal remote sensing, digital terrain models, convolutional neural networks, terrain variability, dataset imbalance, planetary mapping, Lunar Reconnaissance Orbiter**

## I. Introduction

Impact craters are among the most abundant geological features on the lunar surface and serve as important indicators of planetary evolution, surface age, and impact history [1][2]. Accurate crater identification is therefore essential for planetary mapping, geological analysis, landing site assessment, and future lunar exploration missions [3].

Traditional crater identification methods rely heavily on manual interpretation of optical imagery, a process that is both time-consuming and subjective [4]. Advances in machine learning and deep learning have enabled automated crater detection systems capable of processing large volumes of planetary remote sensing data with improved efficiency and consistency [5][6].

Recent studies have increasingly explored the use of multimodal datasets for crater detection. Optical imagery provides information regarding surface texture, albedo variations, and crater morphology, while Digital Elevation Models (DEMs) and Digital Terrain Models (DTMs) capture the topographic characteristics of impact structures [4][6]. Combining these complementary data sources through multimodal fusion has been reported to improve crater detection performance across a variety of planetary environments [7][8][9].

Despite these advances, an important challenge remains insufficiently explored: the ability of crater detection models to generalize across geologically distinct terrains [10][11]. Lunar maria and highland regions exhibit substantial differences in surface morphology, crater preservation state, topographic roughness, and geological history. Consequently, models trained on one terrain type may struggle when applied to another [12].

This study investigates the influence of terrain variability on multimodal lunar crater classification using co-registered optical imagery and DTM data from Mare Tranquillitatis and the Tycho Highlands. Four classification approaches are evaluated, including Optical-only, DTM-only, Early Fusion, and Late Fusion models. In addition to overall classification performance, terrain-specific analyses are performed to assess model robustness across contrasting lunar environments.

The primary contributions of this work are:

- Development of a manually curated multimodal lunar crater dataset containing optical and DTM image patches from geologically distinct lunar terrains.
- Comparative evaluation of Optical, DTM, Early Fusion, and Late Fusion classification approaches under a unified experimental framework.
- Investigation of terrain-dependent generalization through separate evaluation on mare and highland environments.
- Identification of terrain-specific sample imbalance as a major factor influencing crater classification performance.

## II. Study Area and Data

### A. Study Areas

Two geologically distinct lunar regions were selected to investigate the influence of terrain variability on crater classification performance: Mare Tranquillitatis and the Tycho Highlands.

Mare Tranquillitatis is a basaltic mare environment characterized by relatively smooth surfaces, low topographic relief, and well-preserved impact craters. Such terrains provide favorable conditions for crater identification due to their comparatively homogeneous morphology and reduced surface roughness [13]. In contrast, the Tycho Highlands represent a rugged highland environment containing complex topography, overlapping impact structures, elevated surface roughness, and substantial geomorphological heterogeneity [14]. The strong geological contrast between these regions provides a suitable testbed for evaluating the robustness and generalization capability of machine learning models across different lunar terrains.

### B. Data Sources

Multimodal lunar data consisting of optical imagery and Digital Terrain Model (DTM) products were obtained from the Lunar Reconnaissance Orbiter Camera (LROC) Narrow Angle Camera (NAC) DTM archive [15]. Two NAC DTM products were selected for analysis: *NAC_DTM_TRANQPIT1_M155016845_2M*, covering Mare Tranquillitatis, and *NAC_DTM_TYCHOPK04*, covering the Tycho Highlands [16][17].

The optical imagery provides information related to surface texture, albedo, and crater morphology, while the DTM provides elevation-based topographic information associated with impact structures [6]. The NAC DTM products contain co-registered optical and elevation datasets, enabling direct pixel-level correspondence between reflectance and terrain information. This multimodal configuration allows the investigation of both single-modality and fusion-based crater classification approaches.

### C. Patch Extraction and Dataset Curation

Image patches of size $128 \times 128$ pixels were extracted from the selected study regions, consistent with patch-based crater analysis frameworks [7]. Candidate patches were generated from the co-registered optical and DTM datasets to capture a diverse range of crater and non-crater surface features [5].

An initial set of 2,266 candidate patches was produced. To improve label reliability, all candidate patches were manually inspected and assigned binary labels indicating the presence or absence of a crater. Samples exhibiting ambiguous crater morphology, poorly defined structures, partial crater boundaries, or uncertain visual interpretation were removed during quality control.

Following manual curation, 1,904 high-quality samples were retained for subsequent experiments. The resulting dataset contains crater and non-crater examples from both mare and highland terrains, enabling the evaluation of classification performance under substantially different geomorphological conditions. The overall workflow adopted in this study is illustrated in Fig. 1.

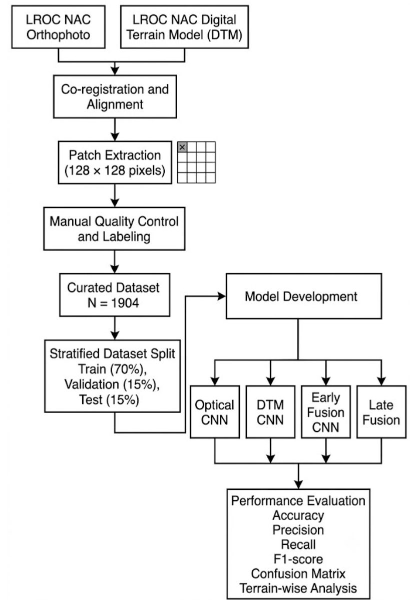


Fig. 1. Overview of the dataset preparation and experimental workflow used in this study. Co-registered optical and DTM products were used for patch extraction, manual labeling, dataset curation, model development, and performance evaluation.

### D. Dataset Partitioning

The curated dataset was divided into training, validation, and testing subsets using a stratified 70:15:15 split. Stratification preserved the overall crater and non-crater class distribution across all subsets to ensure consistent model development and evaluation.

The final partitioning resulted in 1,332 training samples, 286 validation samples, and 286 testing samples. Table I summarizes the dataset partitioning used throughout this study.

TABLE I
Dataset partitioning used for model development and evaluation.

| Subset | Percentage (%) | Samples |
|---|---|---|
| Training | 70 | 1332 |
| Validation | 15 | 286 |
| Testing | 15 | 286 |
| Total | 100 | 1904 |

### E. Dataset Statistics

Table II summarizes the distribution of crater and non-crater samples across the two study regions following manual quality control.

A substantial disparity in crater occurrence was observed between the selected terrains. Mare Tranquillitatis contributed 681 crater samples, whereas only 40 crater samples were identified within the Tycho Highlands. Conversely, the Tycho Highlands contained a large number of non-crater samples associated with rugged terrain, overlapping impact structures, and complex surface morphology.

The low number of verified crater samples in the Tycho Highlands does not imply a lack of impact structures in the region. Rather, it reflects the increased morphological complexity, overlapping crater boundaries, and ambiguous terrain features that prevented reliable manual labeling under the adopted quality-control criteria [14].

This terrain-dependent distribution introduces a challenging classification scenario in which crater availability varies significantly between geological environments. Consequently, the dataset provides an opportunity to evaluate the robustness and generalization capability of crater classification models under substantially different lunar surface conditions.

TABLE II
TERRAIN-WISE DISTRIBUTION OF CURATED SAMPLES.

| Terrain | Crater | Non-Crater | Total |
|---|---|---|---|
| Mare Tranquillitatis | 681 | 452 | 1133 |
| Tycho Highlands | 40 | 731 | 771 |
| Total | 721 | 1183 | 1904 |

## III. METHODOLOGY

### A. Experimental Framework

The objective of this study was to investigate the relative contributions of optical imagery and topographic information for lunar crater classification and to evaluate whether multimodal fusion improves classification performance across contrasting lunar terrains.

Four classification approaches were evaluated:

- **Optical Model** – trained using optical imagery only.
- **DTM Model** – trained using Digital Terrain Model (DTM) data only.
- **Early Fusion Model** – trained using optical and DTM data concatenated as a two-channel input image.
- **Late Fusion Model** – implemented through decision-level fusion by combining the output probabilities of independently trained Optical and DTM models.

All approaches were evaluated using identical training, validation, and testing subsets to ensure a fair comparison between modalities and fusion strategies.

### B. CNN Architecture

To isolate the effect of input modality, all models employed the same lightweight Convolutional Neural Network (CNN) architecture [5][18].

The network consisted of three convolutional layers containing 32, 64, and 128 filters respectively, each using $3\times3$ kernels and Rectified Linear Unit (ReLU) activation functions. Max-pooling operations with a $2\times2$ window were applied after the first two convolutional layers to reduce spatial dimensionality.

A Global Average Pooling layer was used to aggregate spatial features, followed by a fully connected layer containing 64 neurons. A dropout layer with a dropout rate of 0.5 was employed to reduce overfitting. The final output layer consisted of a single neuron with sigmoid activation, producing the probability of crater presence within the input patch. Table III summarizes the model configurations evaluated in this study.

TABLE III
CNN ARCHITECTURE USED FOR ALL CLASSIFICATION MODELS.

| Layer | Output Dimensions |
|---|---|
| Conv2D (32 filters, $3 \times 3$) | $126 \times 126 \times 32$ |
| Max Pooling ($2 \times 2$) | $63 \times 63 \times 32$ |
| Conv2D (64 filters, $3 \times 3$) | $61 \times 61 \times 64$ |
| Max Pooling ($2 \times 2$) | $30 \times 30 \times 64$ |
| Conv2D (128 filters, $3 \times 3$) | $28 \times 28 \times 128$ |
| Global Average Pooling | 128 |
| Dense (64 neurons) | 64 |
| Dropout (0.5) | 64 |
| Dense (1 neuron, sigmoid) | 1 |

### C. Data Normalization

Input data were normalized using statistics computed exclusively from the training subset to prevent information leakage.

For the Optical and DTM models, z-score normalization was applied independently according to

$$x' = \frac{x - \mu}{\sigma} \tag{1}$$

where $x$ represents the original pixel value, $\mu$ denotes the training-set mean, and $\sigma$ denotes the training-set standard deviation.

For the Early Fusion model, optical and DTM channels were normalized independently prior to channel concatenation. This approach preserves modality-specific feature distributions while ensuring comparable numerical scales between channels.

Validation and testing datasets were normalized using the corresponding training-set statistics.

### D. Class Imbalance Handling

The curated dataset exhibited class imbalance, particularly within the Tycho Highlands subset where crater samples were substantially less frequent than non-crater samples.

To mitigate bias toward the majority class during training, class weights were computed using the balanced weighting strategy implemented in the Scikit-Learn framework [19]. These weights were incorporated directly into the binary cross-entropy optimization process.

### E. Training Procedure

All CNN models were trained using the Adam optimizer with binary cross-entropy loss.

Training was performed for a maximum of 20 epochs using a batch size of 32. Early stopping was employed to reduce overfitting, using validation loss as the monitoring metric with a patience value of five epochs.

The model achieving the lowest validation loss was automatically restored and retained for final evaluation.

### F. Early Fusion Strategy

The Early Fusion model utilized a two-channel input representation consisting of co-registered optical imagery and DTM data. The optical and elevation channels were concatenated prior to network input, allowing the CNN to learn joint feature representations directly from both modalities.

This strategy represents feature-level fusion, where cross-modal relationships are learned during feature extraction [7][8][20].

### G. Late Fusion Strategy

To evaluate decision-level multimodal fusion, a Late Fusion model was implemented using the independently trained Optical and DTM classifiers [20][21].

For each test sample, the predicted crater probabilities from the Optical model ($P_{optical}$) and DTM model ($P_{DTM}$) were averaged according to

$$P_{fusion} = \frac{P_{optical} + P_{DTM}}{2} \tag{2}$$

The final class label was obtained using a classification threshold of 0.5.

Equal weighting was selected to provide a simple and transparent decision-level fusion baseline without introducing additional trainable parameters.

This approach preserves modality-specific feature learning while integrating decisions at the prediction stage.

### H. Evaluation Metrics

Model performance was assessed using accuracy, precision, recall, $F_1$-score, confusion matrices, and classification reports.

In addition to overall test-set evaluation, terrain-wise performance analysis was performed separately for Mare Tranquillitatis and Tycho Highlands samples. This analysis was designed to investigate model robustness across contrasting geological environments and to assess the influence of terrain variability on classification performance.

### I. Terrain-wise Evaluation

To examine model generalization across different lunar surface conditions and potential domain shifts, test samples were grouped according to their originating terrain [10][11][12].

Performance metrics were computed independently for Mare Tranquillitatis and Tycho Highlands subsets. This terrain-specific evaluation enabled identification of modality-dependent strengths and weaknesses, as well as potential failure modes associated with geomorphological complexity and terrain-dependent sample availability.

## IV. Results

### A. Overall Classification Performance

Table IV summarizes the performance of the four evaluated approaches on the test dataset.

The DTM, Early Fusion, and Late Fusion models achieved the highest overall accuracy of 75.87%, outperforming the Optical model (75.17%) by 0.70 percentage points. Both Early Fusion and Late Fusion achieved identical accuracies of 75.87%, matching the performance of the DTM-only model. Crater detection performance remained highly consistent across all approaches, with crater $F_1$-scores ranging from 0.74 to 0.75.

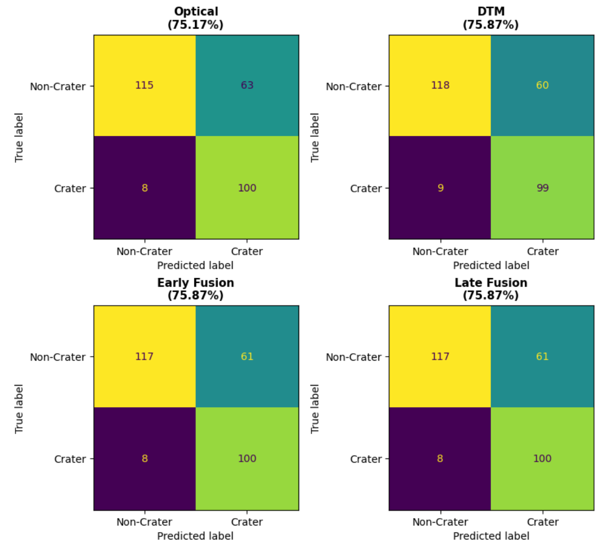


Fig. 2. Confusion matrices for the Optical, DTM, Early Fusion, and Late Fusion models. All approaches exhibit highly similar prediction patterns, with DTM, Early Fusion, and Late Fusion approaches producing nearly identical results.

The relatively small differences between modalities indicate that topographic information provides the dominant discriminative signal for crater classification within the selected study regions [8]. Although multimodal fusion produced a marginal improvement over optical imagery, neither fusion strategy demonstrated a meaningful advantage over the DTM baseline. The similarity of the classification outcomes across all approaches is further illustrated by the confusion matrices shown in Fig. 2.

TABLE IV
OVERALL PERFORMANCE COMPARISON OF THE EVALUATED MODELS.

| Model | Accuracy (%) | Crater $F_1$ |
|---|---|---|
| Optical | 75.17 | 0.74 |
| DTM | 75.87 | 0.74 |
| Early Fusion | 75.87 | 0.75 |
| Late Fusion | 75.87 | 0.74 |

### B. Terrain-wise Performance Analysis

To investigate model generalization across contrasting geological environments, performance was evaluated separately for Mare Tranquillitatis and Tycho Highlands test samples.

The results revealed a strong dependence on terrain type. Within Mare Tranquillitatis, all four models successfully detected the majority of crater samples and achieved crater $F_1$-scores between 0.75 and 0.76. Performance differences between modalities were negligible, with the DTM, Early Fusion, and Late Fusion approaches achieving slightly higher accuracies than the Optical model.

In contrast, all four models failed to identify any crater samples within the Tycho Highlands test subset. Consequently, crater precision, recall, and $F_1$-score were zero across all evaluated approaches despite overall accuracies exceeding 94%.

The terrain-wise results are summarized in Table V.

TABLE V
TERRAIN-WISE CLASSIFICATION PERFORMANCE.

| **Terrain** | **Model** | **Accuracy (%)** | **Crater $F_1$** |
|---|---|---|---|
| Mare | Optical | 61.76 | 0.75 |
| | DTM | 62.94 | 0.76 |
| | Early Fusion | 62.94 | 0.76 |
| | Late Fusion | 62.94 | 0.76 |
| Tycho | Optical | 94.83 | 0.00 |
| | DTM | 94.83 | 0.00 |
| | Early Fusion | 94.83 | 0.00 |
| | Late Fusion | 94.83 | 0.00 |

Although the Tycho Highlands subset exhibited accuracies greater than 94%, these values are misleading because the models classified nearly all samples as non-craters. As a result, the high accuracy primarily reflects the dominance of the non-crater class rather than successful crater detection performance.

### C. Analysis of Fusion Strategies

Both fusion approaches demonstrated performance comparable to the DTM-only model. Early Fusion, implemented through channel concatenation of optical and topographic inputs, achieved identical accuracy to the DTM baseline while improving crater $F_1$-score by only 0.01. Similarly, Late Fusion, implemented through decision-level averaging of Optical and DTM prediction probabilities, produced results nearly indistinguishable from both Early Fusion and DTM-only classification.

These findings suggest that under the current dataset conditions, multimodal fusion contributes limited additional information beyond that already contained within the topographic data. Furthermore, the similarity between Early Fusion and Late Fusion performance indicates that the primary limitation is unlikely to be the fusion strategy itself.

### D. Failure Analysis

The most significant finding of this study is the complete failure of all evaluated models to generalize to crater samples within the Tycho Highlands region [14]. Representative examples from both study regions are shown in Fig. 3.

Following manual quality control, the final dataset contained 681 crater patches from Mare Tranquillitatis but only 40 crater patches from the Tycho Highlands. After dataset partitioning, only six Tycho crater samples were present within the testing subset. Consequently, all models were exposed to substantially more mare crater examples than highland crater examples during training.

The consistent failure observed across Optical, DTM, Early Fusion, and Late Fusion models suggests that terrain-dependent sample scarcity exerted a stronger influence on classification performance than input modality or fusion strategy [10][11]. Despite differences in data representation, all approaches converged to nearly identical predictions within the Tycho subset.

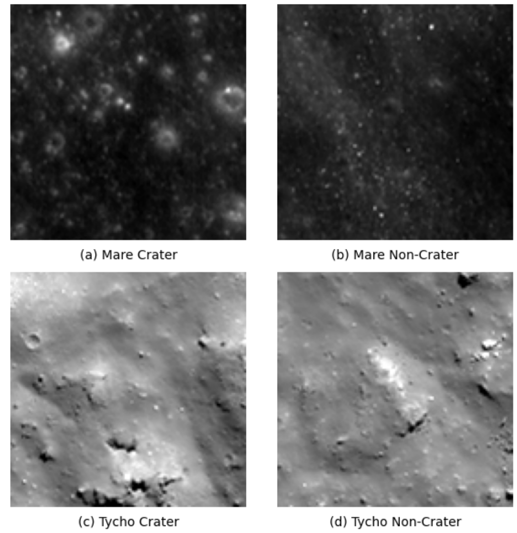


Fig. 3. Representative crater and non-crater patches from Mare Tranquillitatis and Tycho Highlands. Tycho samples exhibit greater morphological complexity and surface roughness than mare samples, illustrating the increased classification difficulty associated with rugged highland terrain.

Consequently, even a single misclassification substantially impacts terrain-specific performance metrics, highlighting the difficulty of robust evaluation under extreme sample scarcity.

These results indicate that robust crater detection across diverse lunar terrains may require more balanced terrain-specific datasets in addition to multimodal information [22]. The findings further suggest that training data diversity may be as important as model architecture when developing generalized lunar crater classification systems.

## V. DISCUSSION

### A. Influence of Input Modality

The comparative evaluation revealed only modest differences between the four investigated approaches. Among the single-modality models, the DTM-based classifier achieved slightly higher performance than the Optical model, suggesting that topographic information provides a more reliable representation of crater morphology than surface reflectance alone [23].

This observation is consistent with the physical characteristics of lunar impact craters and previous reviews of lunar crater detection methodologies [4]. Craters are fundamentally topographic depressions whose geometric structure remains visible in elevation data regardless of illumination conditions. In contrast, optical imagery is strongly influenced by local lighting geometry, shadowing effects, and albedo variations, which may obscure or distort crater boundaries.

Although both Early Fusion and Late Fusion incorporated complementary optical and topographic information, neither fusion strategy produced a substantial improvement over the

DTM-only model. This finding suggests that, within the selected study regions and dataset size, the additional optical information contributed limited discriminative value beyond that already captured by topographic features.

### B. Effectiveness of Multimodal Fusion

Recent studies have reported improvements in crater detection performance through multimodal fusion of optical imagery and elevation data [7][8][9][20][21]. However, the results obtained in this study indicate that the benefits of fusion are highly dependent on data availability, terrain characteristics, and training sample diversity.

The Early Fusion and Late Fusion approaches achieved nearly identical performance and produced confusion matrices similar to those obtained using DTM data alone. These results suggest that the primary limitation was not the fusion strategy itself but rather the characteristics of the available training data.

A possible explanation is that the dataset did not contain sufficient examples of terrain variability for the network to learn robust cross-modal representations. Under such conditions, the models may preferentially rely on the modality containing the strongest and most consistent signal, namely the DTM data.

### C. Terrain-Dependent Generalization

The most significant finding of this study emerged from the terrain-wise evaluation.

All four models achieved reasonable crater detection performance within Mare Tranquillitatis, producing crater $F_1$-scores of approximately 0.75–0.76. However, every model completely failed to identify crater samples within the Tycho Highlands test subset, resulting in a crater recall of zero despite overall accuracies exceeding 94%.

This result demonstrates a substantial terrain-dependent generalization failure [10][11][12]. Although the models successfully learned crater characteristics present within smooth mare environments, they were unable to transfer this knowledge to the morphologically complex highland terrain represented by Tycho [10][11][12].

The Tycho Highlands contain overlapping impact structures, irregular crater morphologies, elevated surface roughness, and complex topographic patterns that differ considerably from the relatively homogeneous mare environment [13][14]. Consequently, crater representations learned from mare-dominated training data may not adequately capture the variability present within rugged highland regions.

### D. Impact of Dataset Imbalance

Analysis of the curated dataset revealed a pronounced imbalance in crater availability between the two study regions. Following manual quality control, 681 crater patches were identified within Mare Tranquillitatis, whereas only 40 crater patches were identified within the Tycho Highlands.

This imbalance persisted throughout the training, validation, and testing subsets despite stratified partitioning. As a result, the models were exposed to substantially more examples of mare crater morphology during training than highland crater morphology.

The Tycho Highlands test subset contained only six crater samples after dataset partitioning. Consequently, terrain-wise performance estimates for this subset should be interpreted with caution and primarily serve as an indicator of generalization behavior rather than a statistically robust performance benchmark.

The consistent failure observed across Optical, DTM, Early Fusion, and Late Fusion models suggests that terrain-dependent sample scarcity exerted a stronger influence on classification performance than the choice of input modality. In other words, the limitation appears to arise primarily from insufficient representation of highland crater examples rather than from deficiencies in the neural network architecture itself.

These findings highlight the importance of terrain-balanced datasets for future lunar crater detection studies [10][23][24]. Increasing the diversity and quantity of crater samples from morphologically complex regions may be necessary to achieve robust generalization across different lunar geological environments.

### E. Limitations and Future Work

Several limitations should be acknowledged.

First, the study considered only two lunar regions, which may not fully represent the diversity of lunar surface conditions. Future investigations should incorporate additional mare and highland sites to evaluate model robustness across a broader range of geological settings.

Second, Only 40 crater samples were identified within the Tycho Highlands compared to 681 crater samples in Mare Tranquillitatis. This resulted in severe terrain-specific imbalance. Expanding highland crater annotations would enable a more rigorous assessment of cross-terrain generalization.

Third, the implemented fusion approaches were intentionally lightweight to facilitate controlled comparison between modalities. More advanced multimodal architectures incorporating attention mechanisms, dual-branch feature extraction, or transformer-based fusion may provide improved integration of optical and topographic information [5][9][20][25][26].

Future work may also investigate one-stage crater detection frameworks based on modern object detection architectures, including lightweight YOLO-based approaches, in addition to transformer and attention-based multimodal fusion strategies [27].

Finally, the present study focused on binary crater classification using fixed-size image patches. Future work could extend this framework toward crater localization and segmentation, enabling automated generation of crater inventories from large-scale lunar datasets.

## VI. Conclusion

This study investigated the effectiveness of optical imagery, Digital Terrain Model (DTM) data, and multimodal fusion strategies for lunar crater classification across two geologically distinct regions: Mare Tranquillitatis and the Tycho Highlands.

Four classification approaches were evaluated, including Optical-only, DTM-only, Early Fusion, and Late Fusion models. Experimental results demonstrated that DTM-based classification slightly outperformed optical imagery, while both fusion strategies achieved performance comparable to the DTM model. The limited improvement obtained through multimodal fusion suggests that topographic information provides the dominant discriminative signal for crater classification within the selected study areas.

Terrain-wise evaluation revealed a substantially more important finding. While all models achieved reasonable performance within Mare Tranquillitatis, every approach failed to detect crater samples within the Tycho Highlands subset. This failure occurred consistently across Optical, DTM, Early Fusion, and Late Fusion models despite their differing input modalities and fusion strategies.

Analysis of the curated dataset indicated that this behavior was strongly associated with terrain-dependent sample imbalance. Following manual quality control, the dataset contained 681 crater patches from Mare Tranquillitatis but only 40 crater patches from the Tycho Highlands. These results suggest that training data distribution exerted a greater influence on classification performance than the choice of input modality or fusion strategy.

Overall, the findings demonstrate that terrain-dependent generalization remains a significant challenge for automated lunar crater classification. While multimodal information can provide complementary observations of crater morphology, robust cross-terrain performance may depend more strongly on the availability of diverse and terrain-balanced training datasets. Future lunar crater detection systems should therefore emphasize both multimodal data integration and improved representation of morphologically complex highland environments.

## Acknowledgments

This work was conducted independently without external funding or institutional support. AI-assisted tools (ChatGPT, Gemini, Consensus, and Anara) were used for language refinement and literature discovery. All scientific interpretations and conclusions were verified by the author.

## References

[1] C. I. Fassett, "Analysis of impact crater populations and the geochronology of planetary surfaces in the inner solar system," *Journal of Geophysical Research: Planets*, vol. 121, no. 10, pp. 1900–1926, 2016.

[2] Y. Wang, B. Wu, H. Xue, X. Li, and J. Ma, "An improved global catalog of lunar impact craters ($\geq$ 1 km) with 3d morphometric information and updates on global crater analysis," *Journal of Geophysical Research: Planets*, vol. 126, no. 9, p. e2020JE006728, 2021.

[3] C. Riedel, *Planetary Surface Evolution from Impact Cratering: A View from Applied Geospatial Methods*. Freie Universitaet Berlin (Germany), 2021.

[4] C. Chaini and V. K. Jha, "A review on deep learning-based automated lunar crater detection," *Earth Science Informatics*, vol. 17, no. 5, pp. 3863–3898, 2024.

[5] A. Silburt, M. Ali-Dib, C. Zhu, A. Jackson, D. Valencia, Y. Kissin, D. Tamayo, and K. Menou, "Lunar crater identification via deep learning," *Icarus*, vol. 317, pp. 27–38, 2019.

[6] X. Lin, Z. Zhu, X. Yu, X. Ji, T. Luo, X. Xi, M. Zhu, and Y. Liang, "Lunar crater detection on digital elevation model: a complete workflow using deep learning and its application," *Remote Sensing*, vol. 14, no. 3, p. 621, 2022.

[7] A. Tewari, V. Verma, P. Srivastava, V. Jain, and N. Khanna, "Automated crater detection from co-registered optical images, elevation maps and slope maps using deep learning," *Planetary and Space Science*, vol. 218, p. 105500, 2022.

[8] Y. Mao, R. Yuan, W. Li, and Y. Liu, "Coupling complementary strategy to u-net based convolution neural network for detecting lunar impact craters," *Remote Sensing*, vol. 14, no. 3, p. 661, 2022.

[9] Y. Dai, C. Xue, and A. Du, "Boosting crater detection via vit-based feature fusion from near-ir images and dems," *IEEE Geoscience and Remote Sensing Letters*, vol. 20, pp. 1–5, 2023.

[10] H. Yang, X. Xu, Y. Ma, Y. Xu, and S. Liu, "Craterdanet: A convolutional neural network for small-scale crater detection via synthetic-to-real domain adaptation," *IEEE Transactions on Geoscience and Remote Sensing*, vol. 60, pp. 1–12, 2021.

[11] S. Yang and Z. Cai, "Progressive domain adaptive network for crater detection," *IEEE Transactions on Geoscience and Remote Sensing*, vol. 60, pp. 1–12, 2022.

[12] Z. Cao, Z. Kang, T. Hu, Z. Yang, L. Zhu, and C. Ye, "Cross-attention induced multilayer domain adaptation network for extraction of sub-kilometer craters from hiric images," *Icarus*, vol. 407, p. 115776, 2024.

[13] M. I. Staid, C. M. Pieters, and J. W. Head III, "Mare tranquillitatis: Basalt emplacement history and relation to lunar samples," *Journal of Geophysical Research: Planets*, vol. 101, no. E10, pp. 23 213–23 228, 1996.

[14] J.-L. Margot, D. B. Campbell, R. F. Jurgens, and M. A. Slade, "The topography of tycho crater," *Journal of Geophysical Research: Planets*, vol. 104, no. E5, pp. 11 875–11 882, 1999.

[15] M. Henriksen, M. Manheim, K. Burns, P. Seymour, E. Speyerer, A. Deran, A. Boyd, E. Howington-Kraus, M. R. Rosiek, B. A. Archinal *et al.*, "Extracting accurate and precise topography from lroc narrow angle camera stereo observations," *Icarus*, vol. 283, pp. 122–137, 2017.

[16] LROC Team, "LROC NAC Digital Terrain Model: Mare Tranquillitatis Pit (TRANQPIT1)," NASA Planetary Data System, 2019, accessed: 2026-05-05. [Online]. Available: https://data.lroc.im-ldi.com/lroc/view_rdr/NAC_DTM_TRANQPIT1

[17] ——, "LROC NAC Digital Terrain Model: Tycho Central Peak (TYCHOPK04)," NASA Planetary Data System, 2014, accessed: 2026-05-05. [Online]. Available: https://data.lroc.im-ldi.com/lroc/view_rdr/NAC_DTM_TYCHOPK04

[18] C. Yang, H. Zhao, L. Bruzzone, J. A. Benediktsson, Y. Liang, B. Liu, X. Zeng, R. Guan, C. Li, and Z. Ouyang, "Lunar impact crater identification and age estimation with chang'e data by deep and transfer learning," *Nature Communications*, vol. 11, no. 1, p. 6358, 2020.

[19] M. Buda, A. Maki, and M. A. Mazurowski, "A systematic study of the class imbalance problem in convolutional neural networks," *Neural networks*, vol. 106, pp. 249–259, 2018.

[20] D. Hong, L. Gao, N. Yokoya, J. Yao, J. Chanussot, Q. Du, and B. Zhang, "More diverse means better: Multimodal deep learning meets remote-sensing imagery classification," *IEEE Transactions on Geoscience and Remote Sensing*, vol. 59, no. 5, pp. 4340–4354, 2020.

[21] J. Yang and Z. Kang, "Bayesian network-based extraction of lunar impact craters from optical images and dem data," *Advances in Space Research*, vol. 63, no. 11, pp. 3721–3737, 2019.

[22] Z. Zhang, Y. Xu, J. Song, Q. Zhou, J. Rasol, and L. Ma, "Planet craters detection based on unsupervised domain adaptation," *IEEE Transactions on Aerospace and Electronic Systems*, vol. 59, no. 5, pp. 7140–7152, 2023.

[23] Y. Juntao, Z. Shuowei, L. Lin, K. Zhizhong, and M. Yuechao, "Topographic knowledge-aware network for automatic small-scale impact crater detection from lunar digital elevation models," *International Journal of Applied Earth Observation and Geoinformation*, vol. 129, p. 103831, 2024.

[24] S. Zang, L. Mu, L. Xian, and W. Zhang, "Semi-supervised deep learning for lunar crater detection using ce-2 dom," *Remote Sensing*, vol. 13, no. 14, p. 2819, 2021.

[25] X. Zhang, J. Lai, Z. Chen, F. Cui, Y. Xu, and X. Zhang, "Dcmwaf-net: Dual cross-modal weighted attention feature fusion network for multiscale lunar crater detection," *IEEE Transactions on Geoscience and Remote Sensing*, vol. 63, pp. 1–20, 2025.

[26] L. Fan, J. Yuan, K. Zha, and X. Wang, "Elcd: Efficient lunar crater detection based on attention mechanisms and multiscale feature fusion networks from digital elevation models," *Remote Sensing*, vol. 14, no. 20, p. 5225, 2022.

[27] R. Yu and Z. Xu, "Crater-masn: A multi-scale adaptive semantic network for efficient crater detection," *Remote Sensing*, vol. 17, no. 18, p. 3139, 2025.